Microscopic nature of inhomogeneous line broadening: Analysis of the excitation-line-narrowing spectra of Cf^{4+} in CeF_4

G. K. Liu, Jin Huang,* and James V. Beitz
Chemistry Division, Argonne National Laboratory, Argonne, Illinois 60439
(Received 14 May 1992; revised manuscript received 4 June 1993)

Optical transitions between $5f$ states of tetravalent californium ion doped (1 metal-atom %) into CeF_4 exhibit unusually large inhomogeneous broadening. The nature of the inhomogeneous broadening in this system has been studied by using fluorescence line narrowing and excitation line narrowing (ELN). It is shown that the energy distributions of different electronic states of Cf^{4+} in this system are correlated. In the ELN experiments, reduced excitation linewidth was obtained when selectively monitoring fluorescence emission. A linear relation was observed between the excitation energies of crystal-field states of the $^5G_{4'}$ manifold and the fluorescence wavelength monitored across the inhomogeneous profile of a $^5G_{6'}-^7F_{6'}$ transition. Analysis of these results by means of a microscopic theory proposed by Laird and Skinner [J. Chem. Phys. **90**, 3880 (1989)] has provided insights into the structural properties of this disordered system.

I. INTRODUCTION

Inhomogeneous broadening in the solid-state spectroscopy of ions or molecules in crystals arises from variation of local environments such as crystalline defects. Traditionally, inhomogeneous broadening has been considered an impediment, because it obscures the observation of detailed energy-level structure or homogeneous linewidths due to various dynamic processes. Many spectroscopic techniques have been developed to eliminate the static effects of inhomogeneous broadening and enable the homogeneous linewidth to be obtained.[1,2] These experimental techniques in turn have given rise to new issues with respect to the effects of structural inhomogeneity on dynamics.[3,4] Recently, attention has been focused on the microscopic nature of inhomogeneous broadening.[4–8] In comparison with the $4f$ state of lanthanide compounds, the $5f$ states of a tetravalent actinide ion are more strongly coupled to host ligands, but still localized. This property of disordered $5f$ systems provides a unique opportunity for investigating the nature of inhomogeneous broadening.

One of the most fundamental issues with respect to the nature of inhomogeneous broadening in solids is the correlation between energies of an ion or molecule and its solid-state environment. It is not always clear if ions with the same transition energy between two states have identical environments or the transition frequencies are accidentally degenerate. Selective spectroscopic experiments such as spectral hole burning or resonant fluorescence line narrowing involving only two states do not provide information with regard to the nature of inhomogeneous line broadening. Experiments that involve a transition between two states followed by a transition to a third state are required to study energy-level correlation in a disordered solid.

Work reported by Sesselmann *et al.*[9] on hole-burning spectra of dye molecules in polymer glasses has shown that both hole position and width are dependent on sample pressure. This work provided evidence that molecules with identical transition energy between two states can have different environments. This result is consistent with a phenomenological model proposed by Lee, Walsh, and Fayer[8] (LWF) in analysis of their fluorescence line narrowing (FLN) and spectral hole-burning (SHB) experiments in organic molecular crystals. In the LWF model, the energy distribution of individual states is completely uncorrelated. If a subset of molecules have the same energy in one state, in a different state they have energies distributed across the whole range of the distribution for that state. As a result, the ions that have the same transition energy between two states can have different local environments. However, there is an alternative view of inhomogeneous line broadening that was first introduced by Motegi and Shionoya[10] and later developed by Selzer, Yen and co-workers[7,11,12] as a phenomenological model of correlated inhomogeneous line broadening. In this model, one assumes that there is a one-to-one correspondence between the energy distribution in one state, and the energy distribution in some other states, i.e., the energy distributions of two different states are completely correlated. In this case, the ions that have the same transition energy between two states must have the same energies in both of the states and thus have the same local environment. Inhomogeneous broadening arises in this model because the energy distribution for two states have different widths. In this case, the nonresonant FLN spectrum is narrowed but may not be as narrow as the resonant FLN line.[7]

In modeling inhomogeneous line broadening, the uncorrelated model and the correlated model represent two extreme cases. In fact, it is widely accepted that there is partial correlation. Residual inhomogeneous broadening was observed in nonresonant FLN studies of many ionic systems.[12–14] In the model of Selzer and Yen,[7,11,12] the concept of accidental coincidence was introduced to interpret the additional broadening found in nonresonant

0163-1829/93/48(18)/13351(10)/$06.00

FLN studies. Recently, Laird and Skinner[5,6] developed a more general statistical theory that describes the microscopic nature of inhomogeneous broadening in a disordered system. They used this theory to interpret the pressure-dependent hole broadening effect in molecular glasses. The correlated Selzer-Yen (SY) model and the uncorrelated LWF model are two limits of the Laird-Skinner (LS) theory.

Studies of energy correlation by means of FLN and excitation line narrowing (ELN) have also been reported for a variety of ions and molecules in glassy hosts.[15–19] We use the term ELN to denote observation of reduced excitation linewidth when selectively monitoring fluorescence emission in comparison with the inhomogeneously broadened absorption profile due to an optical transition between two electronic states. Suter, Wild, and Holzwarth[15] reported evidence of correlation between energies of S_1 and T_1 states of 1-indanones upon $S_0 \rightarrow S_1$ excitation, while no FLN effect was observed when $S_0 \rightarrow S_2$ excitation was conducted. In general, solute-solvent interactions are strongly dependent on the nature of the excited electronic states in glassy matrices which have a wide range of local structure. In most cases, the FLN effect is restricted to the resonant electronic transitions.[16,17] Fluorescence emission of rare-earth ions in inorganic glasses also exhibits substantial inhomogeneous line broadening. In addition to resonant FLN, it was widely observed that the nonresonant emission spectra of Eu^{3+} ions in glasses were narrowed in some degree and the linewidth and position varied as a function of excitation wavelength.[19–22] Sevian and Skinner[23] have recently published a more general theory of inhomogeneous broadening in liquids and glasses and showed that the energy distributions for different states are correlated in a way that depends on the solute-solvent interactions.

Laser selective excitation is very useful in studies of actinide $5f$ spectra in solids; particularly, in heavy actinide doped compounds. Because of radioactivity, samples containing the heavier actinides tend to be contaminated by the decay daughter products, and the resulting radioactivity-induced defects contribute to the observed inhomogeneous broadening. Hessler *et al.*[24] previously investigated $LaCl_3$ doped with Es^{3+} and the energy levels of its decay products, Cf^{3+} and Bk^{3+}, were uniquely determined with selective excitation. In a FLN study of U^{3+}:$LaBr_3$, Hessler *et al.* Observed that only one of the two U^{3+} sites exhibited correlation between excitation and emission energies across the inhomogeneously broadened profiles.[25]

In our previous studies of spectroscopic properties of the $5f$ states of tetravalent actinide ions doped in CeF_4,[26] we focused our attention on both energy-level structure and excited-state dynamics, and reported a photoinduced site distortion process which gives rise to persistent spectral hole burning in these compounds.[27] We measured energy transfer rates that are two orders of magnitude higher than those of $4f$ states of lanthanide systems at the same ion concentration.[28] In our present experiments, we have observed that inhomogeneous line broadening increases with increasing atomic number of the dopant actinide ion. In 1% Cf^{4+}:CeF_4, we have observed nonresonant FLN, excitation line narrowing (ELN), and persistent spectral hole burning. In this paper, we report FLN and ELN experiments that probe the correlation of $5f$ states of Cf^{4+} in CeF_4 and analysis of the data in terms of factors contributing to inhomogeneous line broadening. To our knowledge, this is the first detailed investigation of the nature of inhomogeneous broadening for an actinide compound. Our results are in agreement with the fully correlated limit of the theory of Laird and Skinner.[5,6]

II. EXPERIMENT

The excitation source was a pulsed tunable dye laser (Molectron DL-16P), equipped with a pressure-scanned etalon and grating, pumped by a Q-switched Nd:YAG laser (Quanta Ray DCR-2A). The bandwidth of the dye laser was circa 0.03 cm^{-1} with an etalon in the dye laser oscillator cavity and 0.4 cm^{-1} without an etalon in the cavity. The laser pulse duration was approximately 5 ns and the pulse rate was 10 Hz. Fluorescence from the sample in a variable temperature cryostat (Oxford Instruments CF204) was selected using long pass filters and a 1 m monochromator (SPEX 1704) and detected using a cooled photomultiplier (RCA 31034). Boxcar detectors connected to a computer were used to acquire emission and excitation spectra which were normalized to the dye laser energy using a pyroelectric detector. The optogalvanic effect and an etalon fringe pattern were used to calibrate excitation spectra and to measure the laser bandwidth. The emission spectrum of a neon lamp was recorded to calibrate the Cf^{4+} fluorescence spectra.

Samples were prepared using ^{249}Cf by coprecipitation of Cf^{3+} and Ce^{3+} as fluorides from a solution whose metal content was 1 metal-atom% Cf and 99 metal-atom% Ce. The precipitate was heated in HF gas to generate anhydrous trifluorides, and then in excess F_2 gas to generate the tetrafluoride phase of interest. The resulting powders were sealed off in fused silica tubes containing He gas to ensure good thermal contact.

The host material, CeF_4, is isostructural with UF_4 (Ref. 29) and BkF_4.[30] In these compounds, the metal ion sits on either of two sites, one of C_2 symmetry and the other of C_1 symmetry. There are 12 metal ion sites in one unit cell; 8 metal ion sites are of C_1 symmetry and 4 are of C_2 symmetry. Each metal ion is surrounded by eight fluorine ions arranged in a slightly distorted antiprism configuration. Substitution for Ce^{4+} places Cf^{4+} on sites of C_1 or C_2 symmetry and nonequivalent local environments. Consequently, differences in local environment and energy level structure are expected for Cf^{4+} on the two crystallographically different sites.

To illustrate the origin and termination of the excitation and emission studied in our experiments, a partial energy-level structure of Cf^{4+}:CeF_4 is shown in Fig. 1. For the $5f^8$ configuration of the Cf^{4+} ion in CeF_4, the lowest crystal-field component of the $^5G_6$ multiplet near 15 600 cm^{-1} was the only metastable state from which fluorescence emission was observed. The fluorescence decay was nonexponential at short times following the laser pulse and approached exponential at long times (> 3 μs).

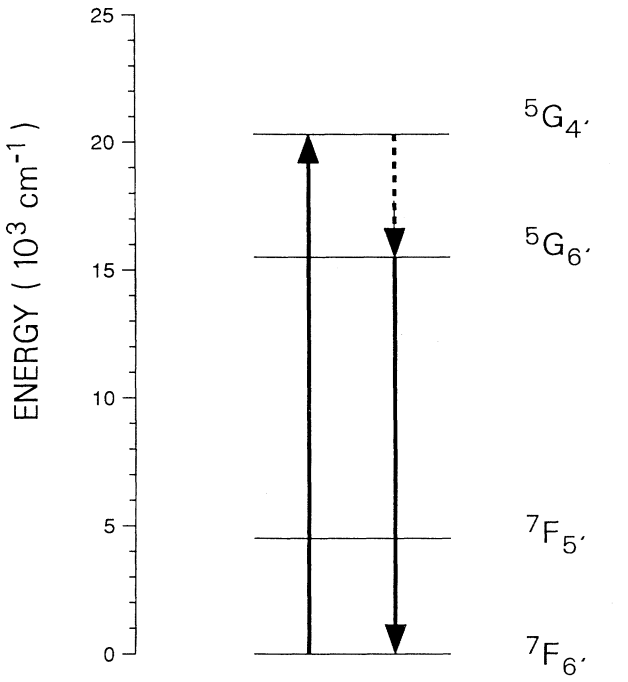

FIG. 1. Partial energy diagram of Cf^{4+} in CeF_4 and optical transitions used in the ELN and FLN experiments.

Fluorescence emission spectra were recorded with 0.5 μs boxcar gate delay and width. Because of the comparable strength of spin-orbit and electron-electron interactions and the considerable J-mixing effect of the crystal field, Russell-Saunder's coupling is not strictly valid for actinide $5f$ states.[26] We denote this by appending a prime to the J value of the term symbol for a given state. Energy levels above $^5G_{6'}$ were probed by scanning the excitation wavelength while monitoring fluorescence emission from $^5G_{6'}$. The first isolated group above the emitting level is $^5G_{4'}$ near 20 300 cm^{-1}. The detailed structure of this group has been studied in the present work.

While the laser was scanned across the energy region of the $^5G_{4'}$ multiplet, the excitation spectra of Cf^{4+} on C_1 and C_2 sites were separated by setting the monochromator (30 cm^{-1} spectral bandpass) to the center of the inhomogeneously broadened emission bands of Cf^{4+} on the C_1 and C_2 sites. Nonresonant FLN was observed when exciting $^5G_{4'}$ and monitoring the emission of the $^5G_{6'} \rightarrow 7F_{6'}$ transition. FLN experiments were carried out on both C_1 and C_2 sites using spectral bandpass as narrow as 1 cm^{-1}. No further attempt to improve resolution was made because no emission band narrower than 2 cm^{-1} was observed in this system even at 4 K. An unusual phenomenon related to nonresonant fluorescence line narrowing was found in this compound. The excitation spectra recorded as the laser wavelength was scanned across the inhomogeneously broadened crystal-field components of the $^5G_{4'}$ level depended on the spectral bandpass and center wavelength of the monochromator selecting transitions between the $^5G_{4'}$ and $^7F_{6'}$ multiplets. As noted above, we call this phenomena excitation line narrowing (ELN) because selective monitoring of fluorescence results in a line-narrowed excitation spectrum. Resonant FLN was not practicable because of the intense scattering of the excitation laser light from the powder sample. The experimental results are summarized and analyzed in the following.

III. SUMMARY OF EXPERIMENTAL RESULTS

A. Site-resolved spectra

Because of large inhomogeneous broadening, optical transitions of the Cf^{4+}:CeF_4 are so broad that the crystal-field splittings of the two crystallographically intrinsic sites could not be resolved in excitation spectra except by selecting a narrow range of fluorescence wavelengths. The broken curve in Fig. 2 shows a part of the excitation spectrum of the $^5G_{4'}$ multiplet obtained when the emission from the $^5G_{6'}$ level ot the ground state was recorded. In our experiment, a bandpass filter was used to reduce scattered laser light and the long wavelength emission to the low-lying excited states. Selective laser excitation was then used to unravel the spectra of the Cf^{4+} on the two crystallographically nonequivalent sites C_1 and C_2. Because of the low symmetry sites, no selection rules are expected in the transitions between crystal-field states.

Although no unique identification could be made with respect to the symmetry of the site of origin based on the experimental measurement alone. Since there are twice

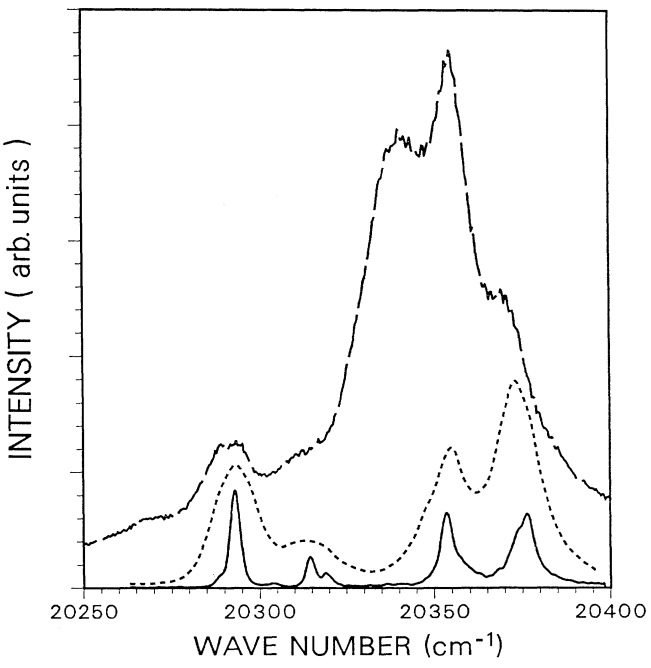

FIG. 2. Site-resolved excitation spectra for the lowest-lying crystal-field components of the $^5G_{4'}$ manifold of Cf^{4+} in CeF_4. The broken curve shows the spectrum without site selection. The dashed curve shows the spectrum for C_2 site, and the solid curve is the ELN spectrum discussed in text. The sample temperature was 12 K for these spectra.

as many C_1 as C_2 sites, we assume that the more intense lines arise from Cf^{4+} on the C_1 site. Besides the spectra of Cf^{4+}, the site selective spectra of Cm^{4+} and Bk^{4+} in the same host also showed that the lines of one site were stronger than the lines of the other site.[28,31] On the average, the magnitudes of lines in the excitation spectra of one site were half of that of the other site. Assuming that Cf^{4+} randomly substitutes for Ce^{4+} (i.e., no special preference for occupying C_1 or C_2 sites), we thus assigned the site resolved spectra to Cf^{4+} on C_1 and C_2 sites according to their relative intensities. In the spectrum of the transitions from the emitting $^5G_6$ multiplet to the ground state, the inhomogeneous emission line centered at 15 524 cm^{-1} was assigned to Cf^{4+} on the C_1 site, and that centered at 15 596 cm^{-1} was assigned to Cf^{4+} on the C_2 site. Alternative assignment was considered based upon the possibility that the oscillator strength of C_2 could be greater than that of the C_1 site for all of the observed transitions from the ground state to the excited states of the Cf^{4+} ion. The dashed curve in Fig. 2 shows the spectrum of the C_2 site that was obtained when the monochromator was centered at 15 596 cm^{-1} and its slits were set to provide a 30 cm^{-1} spectral bandpass. The solid curve in Fig. 2 shows the line-narrowed spectrum obtained at a 1.5 cm^{-1} spectral bandpass. Details of the ELN spectra are discussed in Sec. III C.

The observed excitation and emission spectra consisted of purely electronic transitions as well as vibronic bands associated with each of the two nonequivalent ion sites. The peak intensity of the typically 500 cm^{-1} wide vibronic transitions was generally comparable to, or even stronger than, that of the associated purely electronic zero-phonon lines.

B. Correlation of the ionic radius and inhomogeneous broadening

We have observed a trend in the inhomogeneous broadening of the $5f$-$5f$ transitions of the tetravalent actinide ions An^{4+} (An=Cm, Bk, and Cf) doped into CeF_4. The observed optical linewidth increases with increasing atomic number of the dopant actinide ion. Whereas the full width at half maximum intensity (FWHM) of zero phonon lines for different transitions in the spectra of a 0.1% Cm^{4+} sample and a 5% Cm^{4+} sample are 3–5 cm^{-1},[27,28] the zero phonon lines for the 1% Cf^{4+}:CeF_4 system, as measured in the present work, are 14 cm^{-1} or broader. The zero phonon lines of 0.1% Bk^{4+}:CeF_4 are in a range from 9 to 12 cm^{-1}. Although, there may exist a number of different mechanisms contributing to the observed inhomogeneous line broadening, such as radiation damage, the observed systematic trend in line broadening correlates with the reduction in ionic radius of the dopant tetravalent actinide ion with increasing atomic number. This correlation likely arises because free-ion interactions (including electrostatic interaction and spin-orbit coupling) and crystal-field interaction are a function of the ionic radius (radial distribution of f-electron orbitals). In addition, ionic radius has a critical influence on crystallographic structure and formation of defects that contribute to inhomogeneous broadening. Since the actinide ions studied have a smaller radius than that of the Ce^{4+} host ion, the actinide ions evidently can occupy a variety of sites slightly distorted from the intrinsic C_1 or C_2 sites. The site distortion may be a dislocation of the actinide ion position or structural deformation of the coordination of the surrounding fluoride ions. This effect becomes more significant for the heavier actinide ions since their effective radius is smaller than that of the lighter ones. Figure 3 shows the variation of the effective ionic radius and the observed inhomogeneous linewidth of zero phonon lines for three different actinide ions in CeF_4. The effective ionic radii for the tetravalent ions with a coordination number of 8 are from the work of Shannon.[31]

In a crystal-field analysis of actinide tetrafluorides,[26] it was shown that large crystal-field splittings of the $5f$ states of the tetravalent actinide ions reflect much stronger ion-ligand interactions in these compounds than that in trivalent actinide and lanthanide compounds. Consistent with this result, we observed large inhomogeneous line broadening induced by crystalline defects in the host. In studies of inhomogeneous broadening, the relationship between structural distortion and the energy perturbation in a given system is of interest, particularly, when it is possible to establish a microscopic model for the energy-level distribution on the basis of impurity-defect interactions.

C. ELN spectra

Nonresonant fluorescence line narrowing in 1% Cf^{4+}:CeF_4 was first observed in our experiments when the 20 293 cm^{-1} crystal-field component of the $^5G_4$ multiplet was excited using the narrow band dye laser. At 12 K, the width of the 15 596 cm^{-1} emission band was 16 cm^{-1} when the excitation laser was tuned to a vibronic band in the higher-energy region of the $^5G_4$ manifold. The observed emission linewidth reduced to 2 cm^{-1} when

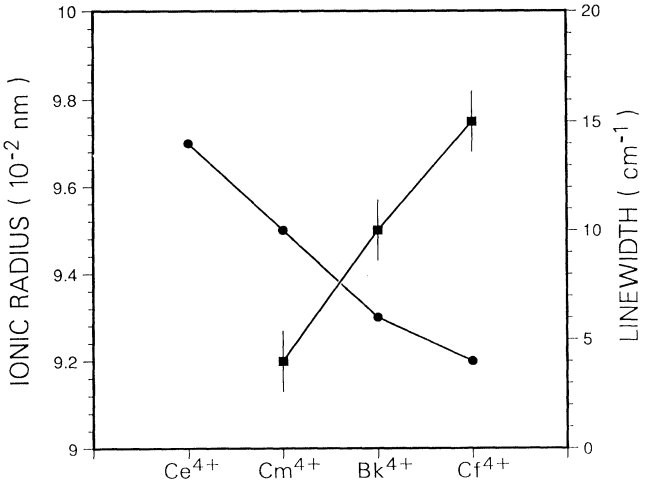

FIG. 3. Comparison of the effective ionic radius of some tetravalent ions (Ref. 31) (●) and the observed inhomogeneous linewidth (■) for tetravalent actinide ions in CeF_4.

using 20 293 cm^{-1} excitation.

In our excitation experiments, the width of the 20 293 cm^{-1} excitation line was 14 cm^{-1} when the monochromator was centered at 15 596 cm^{-1} with a 30 cm^{-1} bandpass. The band centered at 15 596 cm^{-1} corresponds to the emission from the lowest crystal-field component of $^5G_{6'}$ to $^7F_{6'}$, the ground state. The recorded linewidth of the excitation line centered at 20 293 cm^{-1} was 2.4 cm^{-1} when the monochromator was centered at 15 596 cm^{-1} with its slits set to provide 1.5 cm^{-1} spectral bandpass. As shown in Fig. 4, the shapes of the nonresonant ELN and FLN lines are fit by the Lorentzian line-shape function. We obtained similar results for the Cf^{4+} on C_1 sites when the monochromator was centered at 15 524 cm^{-1}.

We also observed that the peak position of lines in the ELN spectrum shifted linearly as a function of the fluorescence wavelength being monitored (i.e., when the monitored fluorescence wavelength was varied across the inhomogeneously broadened $^5G_{6'}$ emission band centered at 15 596 cm^{-1}). A similar effect in the fluorescence spectra of U^{3+}:$LaBr_3$ and Bk^{4+}:CeF_4 was previously observed.[25,32] In our experiments, a set of ELN spectra for the $^5G_{4'}$ group from 20 250 cm^{-1} to 20 400 cm^{-1} were obtained at different emission wavelengths. The ELN spectra shown in Fig. 5 correspond to three different fluorescence energies. This result provides evidence that the energy states of the $^5G_{4'}$ multiplet and the $^5G_{6'}$ emitting state are correlated under the inhomogeneous broadening in this system. The five most prominent lines in the ELN spectrum [c.f. Fig. 5(b)] are accounted for by purely electronic transitions of Cf^{4+} and the weak lines are attributed to accidental coincidence with Cf^{4+} on other defects or trap sites. The asymmetric line shapes for the higher-energy lines are attributed to overlap with vibronic bands associated with the lower-lying states. For higher-energy lines associated with the $^5G_{4'}$ multiplet, no narrowed lines were obtained in the energy region above 20 500 cm^{-1} because of the dominant vibronic structure in this region.

The measured linewidth was 2.4 cm^{-1} for the 20 293 cm^{-1} line at 10 K. Besides the laser bandwidth (0.4 cm^{-1}) and the detection system spectral bandpass (1.5 cm^{-1}), the contributions to the measured linewidth include the homogeneous linewidths of the $^7F_{6'} \rightarrow {}^5G_{4'}$ and $^5G_{6'} \rightarrow {}^7F_{6'}$ transitions and the residual inhomogeneous broadening induced by the accidental degeneracy in energies of the two transitions. The sum of the homogeneous

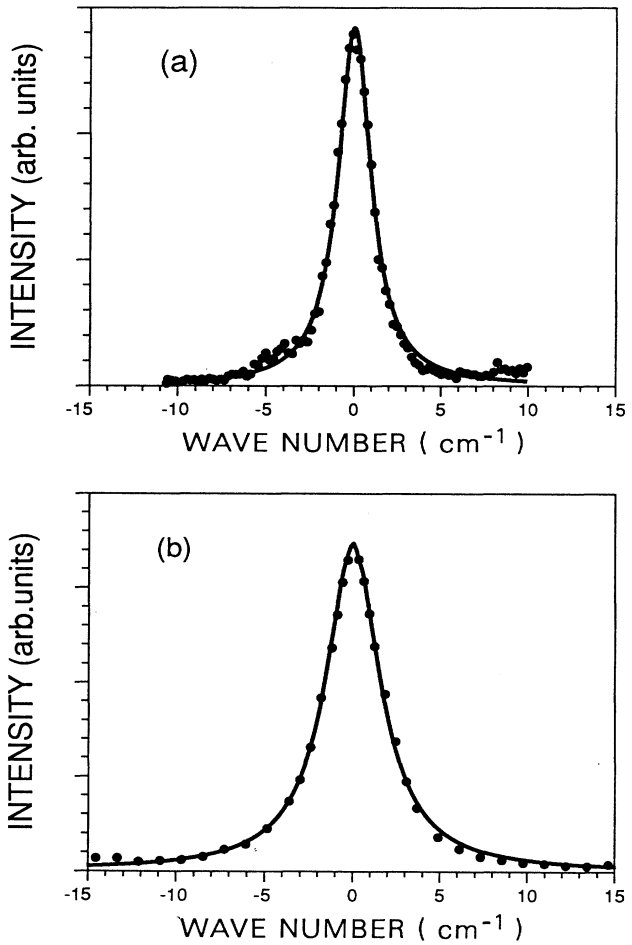

FIG. 4. Observed ELN and FLN spectra fit by a Lorentzian line shape function (shown as a solid line). (a) is the ELN spectrum of the line centered at 20 293 cm^{-1} with the sample at 10 K. Its fit linewidth is 2.4 cm^{-1}. (b) is the FLN spectrum of the emission line at 15 596 cm^{-1} following narrow bandwidth excitation of the 20 293 cm^{-1} line with the sample at 15 K. The fit linewidth is 4 cm^{-1}, and the instrument resolution was 2 cm^{-1}.

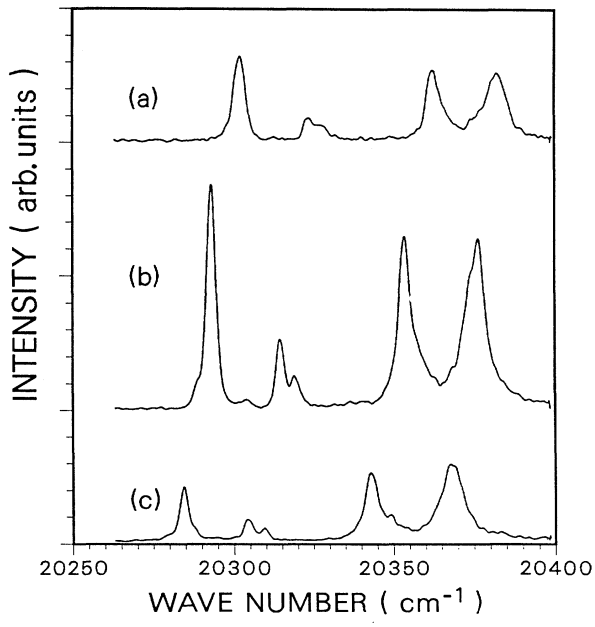

FIG. 5. ELN spectra of the low-lying crystal-field components of the $^5G_{4'}$ manifold of Cf^{4+} on the C_2 site as a function of emission wavelength from $^5G_{6'}$ with the sample 12 K. For spectrum (a) emission was monitored at 15 605.9 cm^{-1}, for (b) at 15 596 cm^{-1}, and for (c) at 15 586.6 cm^{-1}. The spectral bandpass was 2 cm^{-1} for these spectra.

linewidths is estimated to be less than 1 cm^{-1} including possible residual inhomogeneous broadening of the $^7F_{6'} \rightarrow {}^5G_{4'}$ and $^5G_{6'} \rightarrow {}^7F_{6'}$ transitions. Here, we assume that the nonradiative $^5G_{4'} \rightarrow {}^5G_{6'}$ relaxation does not contribute to the line broadening of the two transitions.

It was shown that accidental coincidence gives rise to inhomogeneous broadening in nonresonant FLN spectrum.[7,12] In our case, the "true" homogeneous linewidths for the two transitions we studied are unknown. The measured linewidth from the nonresonant ELN studies could include residual inhomogeneous broadening in the two transitions that involve three electronic states of the Cf^{4+} ion. However, the Lorentzian shape and the temperature dependence of both the FLN and ELN lines suggest that the residual inhomogeneous broadening due to accidental degeneracy should be less than 1 cm^{-1}. In comparision with the overall inhomogeneous linewidth of 14 cm^{-1} for the $^7F_{6'}$ to $^5G_{4'}$ transition, and even broader widths for other transitions, residual inhomogeneous broadening is neglected in the following analysis of the ELN spectra.

IV. MICROSCOPIC THEORY OF INHOMOGENEOUS BROADENING

We consider a crystalline solid containing dilute impurity ions, characterized by a set of electronic states $\{\alpha\}$. In the absence of defect perturbation, all impurity ions have the same energy, E_α^0, as determined by free-ion and crystal-field interactions. Suppose that there exists a large number of static defects such as site dislocations and interstitials in the crystal. The interaction of an impurity ion with each surrounding defect produces a perturbation, $v_\alpha(\mathbf{R})$, on the energy level of the αth state, where $\mathbf{R}$ is the set of relevant defect coordinates (position and orientation). The distribution of defects gives rise to a distribution of absolute energies for a given impurity electronic state.

Inhomogeneous line broadening of a transition from state α to state β is a manifestation of the energy distribution of the two states. In the following, we begin by reviewing the theory of Laird and Skinner[5,6] on the microscopic nature of inhomogeneous broadening in the spectra of impurities. We then extend their treatment to allow direct comparison with our experimental results including those involving three energy states. In the formalism of Laird and Skinner, the inhomogeneous line shape for the transition is described by a convolution of the probability distribution for the energy of state α, $p_\alpha(E)$, and $f_{\beta\alpha}(E'/E)$, the conditional probability that an ion has energy E' in state β given that it had energy E in state α. The energy distribution of state α is obtained from

$$p_\alpha(E)=V^{-N}\int d\mathbf{R}_1\cdots d\mathbf{R}_N P(\mathbf{R}_1,\ldots,\mathbf{R}_N) \times\delta\left[E-\left[E_\alpha^0+\sum_{i=1}^{N} v_\alpha(\mathbf{R}_i)\right]\right], \quad (1)$$

where $P(\mathbf{R}_1,\ldots,\mathbf{R}_N)$ is the probability distribution function for the coordinates of the N defects, normalized to V^N, where V is the volume of the crystal. To obtain Eq. (1), Laird and Skinner[5,6] assumed that the ion-defect interactions are pairwise additive so that the total energy perturbation of a given ion is the sum of the perturbation due to each individual defects. Ion-ion interaction is neglected because of the low concentration.

The conditional probability connecting two states α and β is given by

$$f_{\beta\alpha}(E'/E)=\frac{1}{p_\alpha(E)V^N}\int d\mathbf{R}_1\cdots d\mathbf{R}_N P(\mathbf{R}_1,\ldots,\mathbf{R}_N)\delta\left[E-\left[E_\alpha^0+\sum_{i=1}^{N} v_\alpha(\mathbf{R}_i)\right]\right]\delta\left[E'-\left[E_\beta^0+\sum_{i=1}^{N} v_\beta(\mathbf{R}_i)\right]\right]. \quad (2)$$

Once the energy distribution and conditional probabilities are determined, the transition line shape can be obtained from

$$I_{\beta\alpha}(\Delta E)=\int dE\int dE'\delta(E'-E-\Delta E)f_{\beta\alpha}(E'/E)p_\alpha(E)\ . \quad (3)$$

An approximation made in the LS theory is that the defect coordinates are uncorrelated so that $P(\mathbf{R}_1,\ldots,\mathbf{R}_N)$ can be written[6] as a product of single defect distribution functions $g(\mathbf{R}_i)$

$$P(\mathbf{R}_1,\mathbf{R}_2,\ldots,\mathbf{R}_N)=g(\mathbf{R}_1)g(\mathbf{R}_2)\cdots g(\mathbf{R}_N)\ . \quad (4)$$

Replacing the δ function in Eq. (1) by its integral representation, and defining a new function $J(x)$ by

$$J_\alpha(x)=\int d\mathbf{R}\, g(\mathbf{R})(1-e^{-iv_\alpha(\mathbf{R})x}) \quad (5)$$

then gives the result

$$p_\alpha(E)=\frac{1}{2\pi}\int_{-\infty}^{\infty} dx\, e^{i(E-E_\alpha^0)x}e^{-\rho J_\alpha(x)}\ , \quad (6)$$

where $\rho=N/V$ is the defect density in the system. It is consistent with the observation that for sufficiently large values of the density ρ, the integrand in Eq. (6) is dominated by the values of x for which $J(x)$ is well approximated by the first two terms in its Taylor series about $x=0$. This results in a Gaussian expression for the energy distribution function for state α:

$$p_\alpha(E)=(2\pi D_{\alpha\alpha})^{-1/2}\exp\left[-\frac{(E-E_\alpha)^2}{2D_{\alpha\alpha}}\right], \quad (7)$$

which is centered at

$$E_\alpha=E_\alpha^0+\rho\int d\mathbf{R}\, g(\mathbf{R})v_\alpha(\mathbf{R})\ , \quad (8)$$

with standard deviation $(D_{\alpha\alpha})^{1/2}$, where

$$D_{\alpha\alpha}=\rho\int d\mathbf{R}\, g(\mathbf{R})[v_\alpha(\mathbf{R})]^2\ . \quad (9)$$

With the same approximations made for obtaining $p_\alpha(E)$, the conditional probability connecting the state α and state β is also a Gaussian function:

$$f_{\beta\alpha}(E'/E)=\frac{1}{\sqrt{2\pi(D_{\beta\beta}-D_{\alpha\beta}^2/D_{\alpha\alpha})}}\exp\left[-\frac{[E'-E_\beta-(E-E_\alpha)(D_{\alpha\beta}/D_{\alpha\alpha})]^2}{2(D_{\beta\beta}-D_{\alpha\beta}^2/D_{\alpha\alpha})}\right], \tag{10}$$

centered at

$$E_\beta+(E-E_\alpha)(D_{\alpha\beta}/D_{\alpha\alpha}),$$

and with standard deviation

$$[D_{\beta\beta}-(D_{\alpha\beta}^2/D_{\alpha\alpha})]^{1/2}.$$

The phenomenological SY and LWF models discussed in Sec. I arise naturally as two important limits of the LS theory. First, for potentials such that $D_{\alpha\beta}\ll D_{\alpha\alpha},D_{\beta\beta}$, then

$$f_{\beta\alpha}(E'/E)\approx P_\beta(E'), \tag{11}$$

which is the uncorrelated LWF model.

In some cases, as pointed out by Laird and Skinner,[5] the defect perturbation on the energies of two states has a linear relationship:

$$\nu_\beta(\mathbf{R})=\lambda\nu_\alpha(\mathbf{R}), \tag{12}$$

where λ is a constant. Application of this condition results in $D_{\beta\beta}=D_{\alpha\beta}^2/D_{\alpha\alpha}=\lambda^2D_{\alpha\alpha}$, and Eq. (10) becomes a δ function:

$$f_{\beta\alpha}(E'/E)=\delta[E'-E_\beta-(E-E_\alpha)\lambda], \tag{13}$$

which is the SY model. In this case, the two states are completely correlated. Our results for Cf^{4+}:CeF_4 agree with this limit of the LS theory.

When expressions for $f_{\beta\alpha}(E'/E)$ in Eq. (13) and for $p_\alpha(E)$ in Eq. (7) are substituted into Eq. (3), the following Gaussian line shape for the correlated inhomogeneous broadening is obtained:

$$I_{\beta\alpha}(\Delta E)=\frac{1}{\sqrt{2\pi(1-\lambda)^2D_{\alpha\alpha}}}\times\exp\left[-\frac{[\Delta E-(E_\beta-E_\alpha)]^2}{2(1-\lambda)^2D_{\alpha\alpha}}\right]. \tag{14}$$

The center of the inhomogeneously broadened line is at $E_\beta-E_\alpha$, and the full width at half-maximum (FWHM) of the inhomogeneous line is

$$\Gamma_{\beta\alpha}=2|1-\lambda|\sqrt{2\ln(2)D_{\alpha\alpha}}. \tag{15}$$

Inhomogeneous broadening arises in this model because the variation of the defect-induced potentials for the two states, $\lambda\neq1$, i.e., the energy distributions for the two states have different widths. This is understood based upon the nature of the ion-defect interactions in solids. For example, the magnitude of the electric or magnetic moments of an impurity ion change in different electronic states, but not their directions. This results in that $\nu_\beta(\mathbf{R})=\lambda\nu_\alpha(\mathbf{R})$, where λ is independent of local environment in the system. If $\lambda=1$, there is no inhomogeneous broadening in the transition between the two states, even if there exists a broad distribution of absolute energies in both of the states.

According to the correlated inhomogeneous broadening limit of the LS theory, if a subset of ions initially has the same energy E in state α, they must have the same energy E' in state β so that $E'-E_\beta=(E-E_\alpha)\lambda$. In this case, ions can be selectively excited by a single-frequency laser at energy $\Delta E=E'-E$. However, the ions that have energy $E+\delta$ in the state α have energy $E'+\lambda\delta$ in the state β and, because the energy difference becomes $\Delta E+(\lambda-1)\delta$ between the two states, they cannot be excited by the laser at energy ΔE. In as much as the energy distribution is determined by the defect distribution, the ions that have the same energy should have the same environment. This is why frequency-selective excitation techniques, such as SHB, often have been called site-selective methods.

The other limit of the LS theory corresponds to the uncorrelated LWF model. The LWF model interprets SHB as a degeneracy of transition energies of impurity ions or molecules at different local environments. In this case, energies of impurities are completely uncorrelated between different states. If a subset of ions accidentally have the same energy in state α, they can have their energies in state β distributed as broadly as the entire range of the energy distribution for that state,

$$[f_{\beta\alpha}(E'/E)=p_\beta(E')].$$

Therefore, the ions excited from α to β at the same transition energy can have different absolute energies in both states and, correspondingly, may be sited in different local environments. Usually, line-shape measurements or frequency-selective experiments involving only two electronic states, such as SHB and resonant FLN, are not effective in testing the models corresponding to the extreme limits of the SL theory. Experiments that involve three or more energy states are necessary for resolving the nature of the inhomogeneous broadening.

Let us consider a case similar to our ELN experiments carried out on Cf^{4+}:CeF_4. A narrow band laser excites impurity ions from the ground state α to an excited state β. Following a nonradiative transition from the excited state β to an intermediate state γ, fluorescence emission from γ back to α is monitored. Details of this type of experiment have been given above in Sec. II. We neglect the influence of ion-phonon and ion-ion interactions. We can study the fluorescence line position and shape at a given excitation energy E_e or the excitation line position and shape as a function of the fluorescence energy E_f. The line-shape function can be written as

$$I_{\beta\alpha;\gamma\alpha}(E_e;E_f)=\int dE\int dE'\int dE''\delta(E''-E-E_f)\delta(E'-E-E_e)f_{\gamma\beta\alpha}(E''/E',E)f_{\beta\alpha}(E'/E)p_\alpha(E). \tag{16}$$

where $f_{\gamma\beta\alpha}(E''/E',E)$ is the conditional probability that the ion has energy E'' in state γ, given that it has energy E in state α and E' in state β, $p_\alpha(E)$ is the initial-state distribution, and $f_{\beta\alpha}(E'/E)$ is the conditional probability connecting the α and β states. For a completely correlated system, E' is completely and uniquely determined by E,

$$f_{\gamma\beta\alpha}(E''/E',E)=f_{\gamma\alpha}(E''/E)=f_{\gamma\beta}(E''/E') .$$

Therefore, in this special case, the three-state conditional probability in Eq. (16) can be replaced by a two-state conditional probability, and the line-shape function becomes

$$I_{\beta\alpha;\gamma\alpha}(E_e;E_f)=\int dE \int dE' \int dE''\delta(E''-E-E_f)\delta(E'-E-E_e)f_{\gamma\alpha}(E''/E)f_{\beta\alpha}(E'/E)p_\alpha(E) . \quad (17)$$

Assuming that $\nu_\beta(\mathbf{R})=\lambda\nu_\alpha(\mathbf{R})$, $\nu_\gamma(\mathbf{R})=\lambda'\nu_\alpha(\mathbf{R})$, and using Eqs. (7) and (13), we obtain a line-shape function for the nonresonant fluorescence emission,

$$I_{\beta\alpha;\gamma\alpha}(E_e;E_f)=I_{\beta\alpha}(E_e)|\Phi| \times\delta[(E_e-E_{\beta\alpha})-\Phi(E_f-E_{\gamma\alpha})] , \quad (18)$$

where

$$\Phi=\frac{\lambda-1}{\lambda'-1} \quad (19)$$

represents the ratio of the linewidth for the excitation profile and the linewidth for the emission band. Determined by Eq. (13), $I_{\beta\alpha}(E_e)$ is the value of the line-shape function of $\alpha\rightarrow\beta$ transition at energy E_e, $E_{\beta\alpha}=E_\beta-E_\alpha$ is the center of the $\alpha\rightarrow\beta$ transition, and $E_{\gamma\alpha}=E_\gamma-E_\alpha$ is the center of the $\alpha\rightarrow\gamma$ transition. Therefore, in the case of complete correlation, the emission linewidth is determined by the linewidth of excitation (i.e., the laser linewidth) or the homogeneous linewidth of the $\alpha\rightarrow\beta$ transition whichever is broader.

V. COMPARISON OF THEORY AND EXPERIMENTS

The inhomogeneous broadening of optical transitions in the Cf^{4+}:CeF_4 system is adequately described by the correlated model of inhomogeneous broadening discussed in Sec. IV. Results from the nonresonant FLN and ELN experiments provided evidence of energy correlation between different states of Cf^{4+} in CeF_4. Our ELN experiments on selected Cf^{4+} bands showed that the excitation energy within the inhomogeneous profile linearly related to the fluorescence energy emitted from a lower-lying excited state to the ground state. This one-to-one correspondence in energy levels of different states provides evidence in accord with theory that the ions selectively excited by a narrow band laser have similar local environments in this material.

One limit of the theoretical model of Laird and Skinner, as shown in Sec. IV, predicts a linear relationship between Δ_e, the excitation energy offset from line center, and Δ_f, the fluorescence energy offset from line center [see Eq. (20)]. We have analyzed the ELN spectra for the $^5G_{4'}$ group and obtained a set of data which confirm a linear relationship between Δ_e and Δ_f for five lines in the $^5G_{4'}$ spectrum. The data for four of these lines are shown in Fig. 6. The resulting values of Φ, determined from a linear least squares fit to the ratio of Δ_e/Δ_f for the five lines are listed in Table I.

A nonlinear least-squares method was used to fit the Gaussian line function given in Eq. (14) to each of the five lines primarily contributing to the inhomogeneously broadened excitation profile for the $^5G_{4'}$ multiplet of Cf^{4+} on the C_2 site. The experimental data and the fit spectrum are plotted in Fig. 7. The values of resulting Γ parameter (i.e., FWHM linewidth) for each inhomogeneously broadened line in the spectrum are listed in Table I. The first column in Table I gives the centers of the five inhomogeneously broadened lines. The positions of the line

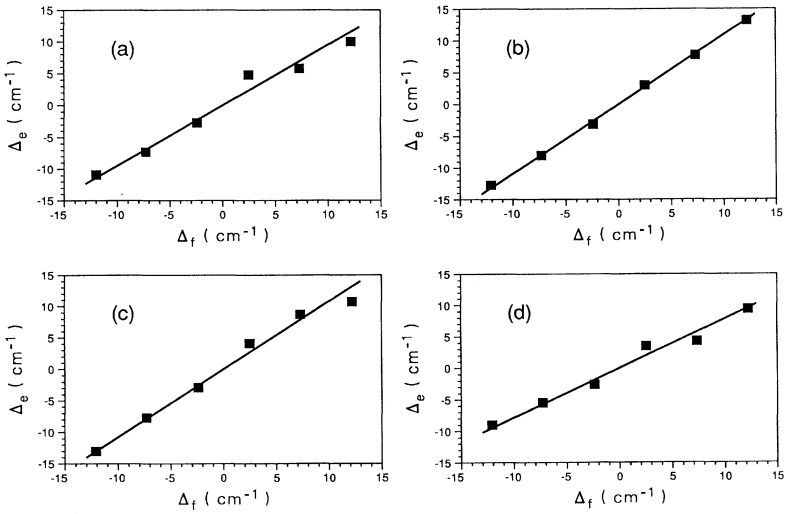

FIG. 6. Comparison of the relationship between step-scanned excitation energy over four crystal-field components of the $^5G_{4'}$ multiplet of Cf^{4+} in CeF_4 and corresponding shifts in the peak emission energy of a $^5G_{6'}$ fluorescence line. In each case, $\Delta_f=0$ corresponds to the center of the 15 596 cm^{-1} emission line. A value of $\Delta_e=0$ in (a) corresponds to the center of the 20 293 cm^{-1} line, in (b) to the center of the 20 314 cm^{-1} line, in (c) to the center of the 20 354.7 cm^{-1} line, and in (d) to the center of the 26 373.5 cm^{-1} line. The solid line in plot is linear least-squares fit to the data points. These spectra were obtained at 12 K.

TABLE I. Linewidth and ELN shift of inhomogeneously broadened $^7F_{6'}-{}^5G_{4'}$ transitions.

Line center E (cm^{-1})	Inhomogeneous linewidth Γ (cm^{-1})	Φ	Γ/Φ (cm^{-1})	$\Gamma_f{}^a-\Gamma/\Phi$ (cm^{-1})
20 293.0	14.0	0.95	14.8	1.2
20 314.0	19.2	1.09	17.6	−1.6
20 318.0	35.4	1.14	31	−15
20 354.7	14.4	1.08	13.3	2.6
20 373.5	15.5	0.78	19.9	−3.9

[a]$\Gamma_f=16$ cm^{-1} is the inhomogeneous linewidth of the 15 596 cm^{-1} emission line measured by using nonsite-selective excitation.

centers were initially set according to the ELN spectrum plotted in Fig. 5(b), and the position of the two upper lines was allowed to varying during the fitting process. The values for Γ were allowed to vary freely in the fitting. The agreement between theory and experiment is excellent for the low energy part of the spectrum (from 20 260 to 20 330 cm^{-1}). However, the Γ value for the third line centered at 20 318 cm^{-1} is exceptionally broad (35.4 cm^{-1}) from the fit. Although, this weak line is broader than the other four lines as evidenced by its larger Φ value obtained from the ELN spectra, the fitting apparently has absorbed contributions from other weak features in this spectral region. A few weak lines appeared in the ELN spectra that have no linear relationship with the emission wavelengths being monitored (see Fig. 6). As discussed in Sec. III D, these features are attributed to accidental coincidence with different defects. Considerable deviation between the observed and calculated spectra in Fig. 7 occurs above 20 330 cm^{-1}. This deviation is attributed to contributions from vibronic transitions built on the electronic energy levels from 20 260 to 20 330 cm^{-1}.

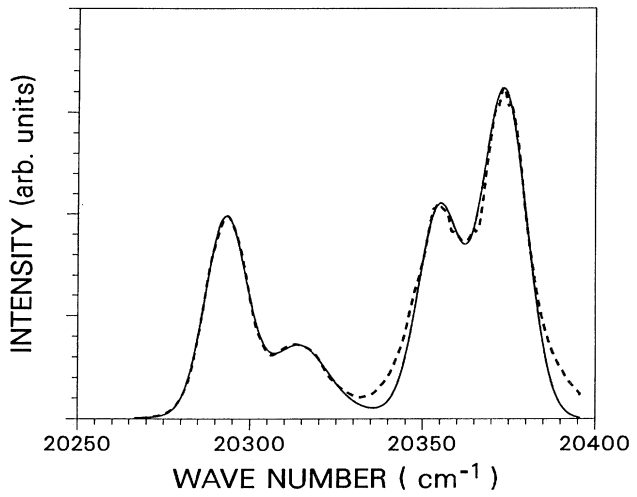

FIG. 7. Comparison of the excitation spectrum (at 12 K) of the lowest-lying crystal-field components of the $^5G_{4'}$ manifold of Cf^{4+} on the C_2 site (dashed line) and a Gaussian line function fit (solid line) to the five purely electronic crystal-field components in this energy range. The divergence between observed and calculated spectra at higher wave numbers is attributed to contributions from vibronic bands lying above 20 330 cm^{-1}.

As an important consequence of the energy correlation, Eqs. (15) and (19) predict that the ratio of the measured linewidth and the slope of the line shift is a constant equal to the linewidth of the emission line. Using the results plotted in Figs. 6 and 7, we have calculated the value of Γ/Φ for the observed electronic lines of the $^5G_{4'}$ multiplet. The results are listed in Table I. For comparison with the Γ/Φ values in Table I, we note that the linewidth for the fluorescence profile of the $^5G_{6'}-{}^7F_{6'}$ transition is 16 ± 1 cm^{-1} measured using 355 nm excitation to avoid site selection. As is evident in Table I, theory and experiment agree, within experimental uncertainties, for the two lowest energy lines in the $^5G_{4'}$ spectrum, whereas the results for other three lines have larger deviations.

VI. CONCLUSIONS

We have studied an interesting system Cf^{4+} in CeF_4, in which optical transitions between $5f$ electronic states are unusually broad. This broadening is a manifestation of strong crystal-field interaction and distribution of a large number of crystalline defects. Energy correlation between different electronic states was observed for most of the Cf^{4+} ion sites coupled to defects in the host. Analysis of the ELN spectra was accomplished with a correlated inhomogeneous broadening model based on a microscopic theory of inhomogeneous broadening in spectra of impurities.

Inhomogeneous line broadening in the 1% Cf^{4+}:CeF_4 system is attributed primarily to the distribution of defect sites created by substituting a smaller ion, Cf^{4+}, for a larger ion, Ce^{4+}, in the CeF_4 lattice. Based on comparison of theory and experiment, we have shown that the distribution of the defect sites and the variation of the static crystal-field levels of the $5f$ states have a correlated relationship in this system. Residual inhomogeneous broadening due to accidental coincidence involving three states in the nonresonant ELN and FLN spectra is small in comparison with the overall inhomogeneous broadening in this system.

Analysis of the frequency-selective spectra of a disordered system provides information on the nature of inhomogeneous line broadening. Using the microscopic theory discussed in Sec. IV, we have established a relationship between crystalline defects and spectral properties in a disordered system in which inhomogeneously broadened energy levels are correlated. The ELN technique we used in the present work is a particularly useful method for probing structural defects of a disordered system in which optical transitions are inhomogeneously broadened. For a system in which the inhomogeneous line broadening is correlated, the ELN method provides a direct measure of the energy-level shift of impurities as a function of defect perturbation, thus enabling the variation of local structure to be determined. Future studies of disordered systems having this property may result in a quantitative description of defect perturbation on the basis of specific impurity-defect interactions.

ACKNOWLEDGMENTS

This work was performed under the auspices of the Office of Basic Energy Sciences, Division of Chemical Sciences, U.S. Department of Energy, under Contract No. W-31-109-ENG-38. We thank C. W. Williams for preparing and characterizing the sample and the transplutonium element production facilities at Oak Ridge National Laboratory for supplying the ^{249}Cf used in this work. We gratefully acknowledge important advice and comments from J. L. Skinner.

*Permanent address: Department of Physics and Astronomy, University of Wisconsin at Eau Claire, Eau Claire, WI 54702.

[1]R. M. Macfarlane and R. M. Shelby, in *Spectroscopy of Solids Containing Rare Earth Ions,* edited by A. A. Kaplyanskii and R. M. Macfarlane (North-Holland, Amsterdam, 1987), p. 51.

[2]W. M. Yen and P. M. Selzer, in *Laser Spectroscopy of Solids,* edited by W. M. Yen and P. M. Selzer (Springer, Berlin, 1981), p. 141.

[3]R. M. Macfarlane, J. Lumin. **45**, 1 (1990).

[4]J. L. Skinner, B. B. Laird, and L. Root, J. Lumin. **45**, 6 (1990).

[5]B. B. Laird and J. L. Skinner, J. Chem. Phys. **90**, 3880 (1989).

[6]B. B. Laird and J. L. Skinner, J. Chem. Phys. **90**, 3274 (1989).

[7]P. M. Selzer, in *Laser Spectroscopy of Solids,* edited by W. M. Yen and P. M. Selzer (Springer, Berlin, 1981), p. 113.

[8]H. W. H. Lee, C. A. Walsh, and M. D. Fayer, J. Chem. Phys. **82**, 3948 (1985).

[9]T. Sesselmann, W. Richter, D. Haarer, and H. Morawitz, Phys. Rev. B **36**, 7601 (1987).

[10]N. Motegi and S. Shionoya, J. Lumin. **8**, 1 (1973).

[11]P. M. Selzer and W. M. Yen, Opt. Lett. **1**, 90 (1977).

[12]R. Flach, D. S. Hamilton, P. M. Selzer, and W. M. Yen, Phys. Rev. B **15**, 1248 (1977).

[13]M. J. Weber, J. A. Paisner, S. S. Sussman, W. M. Yen, L. A. Riseberg, and C. Brecher, J. Lumin. **12/13**, 729 (1976).

[14]L. E. Erickson, Phys. Rev. B **11**, 77 (1975).

[15]G. W. Suter, U. P. Wild, and A. R. Holzwarth, Chem. Phys. **102**, 205 (1986).

[16]H. J. Griesser and U. P. Wild, J. Chem. Phys. **73**, 4715 (1980).

[17]T. Kushida and E. Takushi, Phys. Rev. B **12**, 824 (1975).

[18]A. J. Kallir, G. W. Suter, and U. P. Wild, J. Phys. Chem. **89**, 1996 (1985).

[19]M. J. Weber, in *Laser Spectroscopy of Solids,* edited by W. M. Yen and P. M. Selzer (Springer, Berlin, 1981), p. 189.

[20]C. Brecher and L. A. Riseberg, Phys. Rev. B **12**, 81 (1976).

[21]C. Brecher and L. A. Riseberg, J. Non-Cryst. Solids **40**, 469 (1980).

[22]J. Hegarty, W. M. Yen, and M. J. Weber, Phys. Rev. B **18**, 5816 (1978).

[23]H. M. Sevian and J. L. Skinner, Theor. Chim. Acta **82**, 29 (1992).

[24]J. P. Hessler, J. A. Caird, W. T. Carnall, H. M. Crosswhite, R. J. Sjoblom, and F. Wagner, Jr., in *The Rare Earths in Modern Science and Technology,* edited by G. J. McCarthy and J. J. Rhyne (Plenum, New York, 1979), p. 507.

[25]J. P. Hessler, J. Hegarty, G. G. Levey, G. F. Imbusch, and W. M. Yen, J. Lumin. **18/19**, 73 (1979).

[26]W. T. Carnall, G. K. Liu, C. W. Williams, and M. F. Reid, J. Chem. Phys. **95**, 7194 (1991).

[27]G. K. Liu and J. V. Beitz, Chem. Phys. Lett. **171**, 335 (1990).

[28]G. K. Liu and J. V. Beitz, Phys. Rev. B **41**, 6201 (1990).

[29]A. C. Larson, R. B. Roof, and D. T. Cromer, Acta Cryst. **17**, 555 (1964).

[30]D. D. Ensor, J. R. Peterson, R. G. Haire, and J. P. Young, J. Inorg. Nucl. Chem. **43**, 1001 (1981).

[31]R. D. Shannon, Acta Cryst. A **32**, 751 (1976).

[32]G. Jursich, G. K. Liu, and J. V. Beitz (unpublished).